Hydrotreatment of the carbohydrate-rich fraction of pyrolysis liquids using bimetallic Ni based catalyst

Yin, Wang; Venderbosch, Robertus Hendrikus; Alekseeva, Maria V.; Figueiredo, Monique Bernardes; Heeres, Hans; Khromova, Sofia A.; Yakovlev, Vadim A.; Cannilla, Catia; Bonura, Giuseppe; Frusteri, Francesco

Published in:
Fuel processing technology

DOI:
10.1016/j.fuproc.2017.10.006

Fuel Processing Technology 169 (2018) 258–268

Contents lists available at ScienceDirect

Fuel Processing Technology

journal homepage: www.elsevier.com/locate/fuproc

Research article

Hydrotreatment of the carbohydrate-rich fraction of pyrolysis liquids using bimetallic Ni based catalyst: Catalyst activity and product property relations

Wang Yin[a], Robertus Hendrikus Venderbosch[b], Maria V. Alekseeva[c], Monique Bernardes Figueirêdo[a], Hans Heeres[b], Sofia A. Khromova[c], Vadim A. Yakovlev[c], Catia Cannilla[d], Giuseppe Bonura[d], Francesco Frusteri[d], Hero Jan Heeres[a,*]

[a] Department of Chemical Engineering, University of Groningen, Nijenborgh 4, 9747 AG, Groningen, The Netherlands
[b] Biomass Technology Group BV, Josink Esweg 34, 7545 PN Enschede, The Netherlands
[c] Boreskov Institute of Catalysis, 5, pr. Akad. Lavrentieva, 630090 Novosibirsk, Russia
[d] CNR-ITAE, Istituto di Tecnologie Avanzate per l'Energia "Nicola Giordano", Via S. Lucia sopra Contesse, 5-98126 Messina, Italy

ARTICLE INFO

Keywords:
Pyrolysis liquids
Pyrolytic sugar
Ni based catalysts
Hydrotreatment

ABSTRACT

The use of novel nickel based catalysts for the catalytic hydrotreatment of pyrolytic sugars, the carbohydrate-rich fraction of pine derived pyrolysis liquids, is reported. The catalysts are characterized by a high nickel loading (38 to 57 wt%), promoted by Cu, Pd, and/or Mo and a SiO_2 based inorganic matrix. Experiments were carried out at 180 °C and 120 bar initial hydrogen pressure (room temperature) in a batch reactor set-up to gain insight in catalyst activity and product properties as a function of the catalyst composition. The most promising catalyst in terms of activity, as measured by the hydrogen uptake during reaction, was the Ni-Mo/SiO_2-Al_2O_3 catalyst whereas the performance of the monometallic Ni/SiO_2-Al_2O_3 catalyst was the lowest. As a result, the product oil obtained by the bimetallic Ni-Mo catalyst showed the highest H/C ratio and the lowest molecular weight of all catalysts tested. A detailed catalyst characterization study revealed that addition of Mo to the Ni catalyst suppresses the agglomeration of nickel nanoparticles during the catalytic hydrotreatment reaction.

1. Introduction

Lignocellulosic biomass has been identified as a renewable resource for the production of transportation fuels and biobased chemicals [1,2]. However, biomass logistics are complex and expensive and as such there is a strong incentive to develop cost effective technologies for the densification/liquefaction of biomass. Fast pyrolysis is such a promising technology as it converts lignocellulosic biomass into a vapor phase which is subsequently condensed to obtain a pyrolysis liquid at relatively mild temperatures (450–600 °C) [3,4]. Liquid yields of 70 to 80% on dry biomass input have been reported. However, the pyrolysis liquids are rather acidic (pH usually around 3) [5]. The presence of acids and other reactive oxygenated functional groups renders the liquids relatively polar, and non-miscible with hydrocarbons. Furthermore, thermal stability is limited due to repolymerization of reactive organic compounds [5]. In addition, the energy density is typically < 50% of that of conventional oils due to the presence of water (15–30%) and oxygenates (typical oxygen contents are between 35 and 40%) [6].

Catalytic hydrotreatment has shown to be an attractive technology to obtain stabilized pyrolysis liquids with a tunable oxygen content [5,7]. Various metal-support combinations have been applied either using pyrolysis liquids as such or in combination with a solvent. Early studies on the hydrotreatment of pyrolysis liquids involved the use of conventional hydrodesulfurization catalysts, e.g. sulfided NiMo and CoMo on γ-Al_2O_3, and allowing for for the production of fully deoxygenated products [8]. However, these catalysts have some drawbacks such as (i) the requirement of high temperatures (up to 400 °C), (ii) significant deactivation under the harsh conditions and (iii) requirement of the presence of S for good performance. Noble metal catalysts were also tested extensively (Ru, Pd, Pt, Rh on various supports, e.g. Al_2O_3, TiO_2, active carbon, ZrO_2, etc.) [9,10]. Among these, Ru/C was found to be superior to the classical hydrotreating catalysts with respect to oil yield (up to 60 wt%), though deep deoxygenation in a single step proved not possible [10].

In previous studies on the catalytic hydrotreatment of pyrolysis liquids using a Ru/C catalyst [5], various parallel and consecutive reactions were proposed to explain the product portfolio after the hydrotreatment reaction (Scheme 1). At relatively low temperatures, the desired hydro-(deoxy)genation and undesired thermal, non-catalyzed polymerization reactions occur in parallel. The latter route ultimately

* Corresponding author.
E-mail address: h.j.heeres@rug.nl (H.J. Heeres).

http://dx.doi.org/10.1016/j.fuproc.2017.10.006
Received 10 July 2017; Received in revised form 26 September 2017; Accepted 7 October 2017

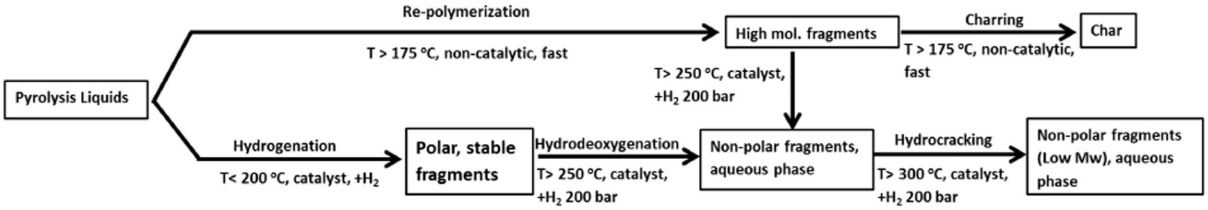

Scheme 1. Proposed reaction pathway for the catalytic hydrotreatment of pyrolysis liquids over Ru/C [5].

Table 1
Relevant properties of the pyrolytic sugars used in this study.

Water content (wt%)	14.46
Elemental composition (dry basis, wt%)	
C	50.80
H	6.35
O (by difference)	42.85
N	< 0.01

leads to char, thus lowering the carbon efficiency of the process and causing operational issues.

It is generally assumed that the sugar fraction of pyrolysis liquids, which is known to contain among others acetol, glycolaldehyde, furfural, furanone, levoglucosan and oligomeric (dehydrated) carbohydrates, is prone to thermal polymerization reactions leading to char (top route in Scheme 1) [5]. Efficient hydrogenation of this sugar fraction into more stable components, e.g. aldehydes and ketones to alcohols and sugars to sugar alcohols, is thus expected to reduce char formation. Experimental studies on related processes have indeed confirmed this statement. For instance, Vispute and et al. [11] reported bio-aromatics production from the sugar fraction of pyrolysis liquids using zeolite catalysts. Coke formation was considerably reduced (from 32.3 down to 12.6%) and aromatics yields increased (from 8.2 up to 21.6%) by first applying a low temperature hydrogenation step of the water soluble phase of the pyrolysis liquids using Ru/C or Pt/C catalysts. Vispute and et al. [12] also reported alkane production from the aqueous phase processing of pyrolysis liquids and showed that prior hydrogenation of the water soluble phase of the pyrolysis liquids at 175 °C using a Ru/C catalyst considerably increased the selectivity to alkanes from 42 to 85%.

Recently, a new series of non-noble metal based catalysts was introduced by our groups for the hydrotreatment of pyrolysis liquids [13]. These catalysts are Ni-based, prepared by as sol-gel method and promoted by among others Cu or Pd, and show clear advantages compared to Ru/C such as (i) low methane formation rates, limiting the consumption of (expensive) hydrogen and (ii) reduced rates of char formation [13]. Ni based catalysts for the catalytic hydrotreatment of pyrolysis liquids have also been reported by other groups [14–17].

As mentioned earlier, primarily the sugar fraction is assumed to be responsible for repolymerization reactions leading to char, which makes it obvious that this fraction should be treated first, and preferably at low temperature (< 180 °C), to obtain a higher quality product oil. We here report the catalytic hydrotreatment of specifically the sugar fraction of pyrolysis liquids over Ni based catalysts with various Ni contents (38–57 wt%), promoters (Pd, Cu and Mo) on a SiO_2 based matrix. A monometallic Ni catalyst was used as a reference catalyst to gain insights in promotor effects.

All experiments were performed using an isolated sugar fraction (pyrolytic sugar) from a representative pyrolysis liquid as the starting material at 180 °C, 120 bar H_2 for 4 h in a batch reactor. These conditions are based on earlier studies from our group on the catalytic hydrotreatment of pyrolysis liquids [5,10,13]. The best catalysts were characterized using a wide range of techniques before and after reaction. Relevant properties of the hydrotreated products such as elemental composition, water content and molecular weight distribution were determined to evaluate catalyst performance.

2. Experimental section

2.1. Materials

The pyrolytic sugar (PS) fraction, obtained from a pine derived pyrolysis liquid, was supplied by the Biomass Technology Group (BTG, Enschede, the Netherlands). The PS fraction was prepared by the addition of water to the pyrolysis liquid, leading to the formation of a viscous oil phase (pyrolytic lignin) and a separate water phase. The water phase was taken and subjected to an evaporation step (75 °C, 100 mbar, till vapor formation ceased) to remove most of the water. The remaining viscous liquid was used for the experiments, and relevant properties are given in Table 1.

Hydrogen, nitrogen and helium were obtained from Linde and were all of analytical grade (> 99.99%). A reference gas containing H_2, CH_4, ethylene, ethane, propylene, propane, CO and CO_2 with known amounts for gas phase calibration was purchased from Westfalen AG, Münster, Germany.

H_2SO_4 (98%) from Merck, glycolaldehyde dimer (crystalline), glucose (≥ 99.5%), mannose (≥ 99%), xylose (≥ 99%), arabinose (≥ 99%), tetrahydrofuran (THF, anhydrous), di-*n*-butyl ether (DBE, anhydrous, 99.3%) were purchased from Sigma-Aldrich and used without further purification, levoglucosan was supplied from Carbosynth, UK and used as received.

2.2. Catalyst synthesis and composition

All catalysts were prepared using a sol-gel method according to a procedure given by Bykova et al. [18–21]. Catalyst compositions (in oxidized state) are presented in Table 2. The catalysts were crushed to 25–75 μm and reduced in situ for 1 h at the temperatures specified in Table 2 before use.

2.3. Experimental procedures

2.3.1. Catalytic hydrotreatment of the pyrolytic sugars in a batch autoclave

Experiments were performed in a 100 mL autoclave (Parr) equipped with an overhead stirrer. Prior to an experiment, the reactor was charged with 1.25 g of catalyst (5 wt% with respect to pyrolytic sugar) and the reactor was pressurized to 100 bar of N_2 to check for leakage.

Table 2
Summary of the catalysts used in this study.[a]

Code	Metal loading, wt%				Support, wt%			Reduction temperature (°C)
	Ni	Cu	Mo	Pd	SiO_2	Al_2O_3	ZrO_2	
Ni	48	–	–	–	15.5	24	–	400
Ni-Cu	46	5	–	–	25	–	10.7	350
Ni-Pd	57	–	–	0.7	26	–	–	350
Ni-Pd-Cu	54	8.2	–	0.7	21	–	–	350
Ni-Mo	41	–	7.4	–	13.3	24	–	400
Ni-Mo-Cu	38	3.8	5.9	–	10.8	24	–	400

[a] In oxidized form.

The catalyst was then activated by applying 20–30 bar H_2 at a temperature of 350–400 °C (see Table 2) for 1 h, after which the reactor was cooled to room temperature and 25.0 g of PS was injected to the reactor from a feed vessel using pressurized nitrogen gas. The reactor was flushed 3 times with 10 bar of hydrogen to remove any remaining air/oxygen, and was subsequently pressurized with hydrogen to 120 bar at room temperature. Finally, the reactor content was heated up to 180 °C with a heating rate of 10 °C/min. The reactor was kept at 180 °C for 4 h while stirring at 1400 rpm and subsequently cooled to ambient temperature. The pressure in the reactor was determined and the gas phase was sampled using a 3 L gas bag. The liquid and solid product (mainly spent catalyst) were collected after reaction and transferred to a centrifuge tube. Both phases were separated by centrifugation (4500 rpm, 30 min) and collected and weighted. The reactor was thoroughly rinsed with acetone. The acetone was evaporated (in air at room temperature), and the resulting product was weighted and added to the liquid phase for mass balance calculation. The suspension was combined with the solid residue in the centrifuge tube, filtered over a paper filter, washed with acetone and water, further dried at 100 °C until constant weight. The amount of char formed is defined as the amount of solid residue minus the original catalyst intake. The amount of gas phase components after reaction was determined by the pressure difference in the reactor before and after reaction at room temperature using the ideal gas law in combination with the measured composition of the gas phase by GC. It is assumed that the volume of the gas hold-up in the reactor before and after reaction is equal. For non-catalytic runs, the pyrolytic sugar was heated in the reactor to 180 °C for 4 h under 120 bar of N_2 gas and samples of the liquid and solid phase after reaction were collected using the same methodology as for the catalytic runs.

2.3.2. Analysis of gas- and liquid phase

2.3.2.1. GC-TCD. The composition of the gas phase after reaction was determined by GC-TCD. A Hewlett Packard 5890 Series II GC equipped with a CP Poraplot Q Al_2O_3/Na_2SO_4 column (50 m × 0.5 mm, film thickness 10 μm) and a CP-Molsieve 5 Å column (25 m × 0.53 mm, film thickness 50 μm) was used. The injector temperature was set at 150 °C, the detector temperature at 90 °C. The oven temperature was kept at 40 °C for 2 min, then heated up to 90 °C at 20 °C/min and kept at this temperature for 2 min. Helium was used as the carrier gas. The columns were flushed for 30 s with reference and sample gas before starting the measurement. A reference gas containing H_2, CH_4, CO, CO_2, ethylene, ethane, propylene and propane with known composition was used for peak identification and quantification.

2.3.2.2. Determination of the composition of the pyrolytic sugar. The composition and particularly the amounts of monomeric and oligomeric sugars were determined using a hydrolysis method [22]. A glass pressure tube was filled with 100 mL of a 500 mM sulphuric acid (98%) solution in water and 1.0 g of pyrolytic sugar. The tube was closed and placed in an oven at the preset temperature (80 and 120 °C) for 24 h. After reaction, the content was cooled to room temperature, the solution was filtered and analyzed using HPLC. The HPLC was equipped with a Hewlett Packard 1050 pump, a Bio-Rad organic acid column (Aminex HPX-87H) and a differential refractometer. The mobile phase consisted of an aqueous solution of sulfuric acid (5 mmol/L) using a flow rate of 0.55 cm^3/min. The column was operated at 60 °C. Quantification of the various products was performed using calibration curves obtained from standard solutions of known concentrations. The amounts of levoglucosan and glycolaldehyde in the pyrolytic sugar fraction were quantified without the hydrolysis step by direct injection of the diluted pyrolytic sugars solution.

2.3.2.3. Calculation of the hydrogen consumption in a batch reaction. The H_2 consumption for each batch experiment was calculated according a literature method [23,24]. It is based on the initial pressure, temperature and composition of the gas phase before and after the reaction. In these calculations, it is assumed that the volume of the gas phase in the reactor is constant and that the ideal gas law is applicable. The initial number of moles of H_2 in the reactor is given by:

$$n_{H_2,initial} = \frac{V_{gas\ cap} \cdot P_{initial}}{R \cdot T_{initial}} \quad (1)$$

where $n_{H_2},initial$ is the initial amount of hydrogen (in moles) in the reactor, $V_{gas\ cap}$ is the volume of the reactor that is not occupied by the liquid, $P_{initial}$ is initial pressure in the reactor (in room temperature), R is gas constant, and $T_{initial}$ is the initial temperature in the reactor (room temperature).

After reaction, the reactor was cooled to room temperature and the pressure was recorded. In combination with the known composition of the gas phase (GC-TCD), the amount of hydrogen at the end of the reaction is given by:

$$n_{H_2,\ final} = y_{H_2,\ final} \times \frac{V_{gas\ cap} \cdot P_{final}}{R \cdot T_{final}} \quad (2)$$

where $n_{H_2},final$ is the amount of hydrogen uptake (in moles) in the reactor after the reaction, $y_{H_2},final$ is the mole fraction of the hydrogen in the gas cap after reaction (as measured by GC-TCD), $V_{gas\ cap}$ is the volume of the reactor that is not occupied by the liquid, P_{final} is the pressure in the reactor after the reaction (measured in room temperature), R is gas constant, T_{final} is the final temperature in the reactor (room temperature).

The hydrogen uptake per kg feed was calculated using Eq. (3).

$$H_2\ consumption = \frac{(n_{H_2,\ initial} - n_{H_2,final}) \cdot \frac{R \cdot 298K}{1\ atm}}{m_{PS,\ initial}} \quad (3)$$

where H_2 *consumption* is the hydrogen uptake (in NL per kg dry feed), $n_{H_2},initial$ is the initial amount of hydrogen (in moles) in the reactor, $n_{H_2},final$ is the amount of hydrogen uptake (in moles) in the reactor after the reaction, R is gas constant, $m_{PS,\ initial}$ is the mass of the pyrolytic sugar fraction fed to the reactor.

2.3.2.4. Elemental analysis. The elemental composition of the pyrolytic sugar feed and the product oils were analyzed using a EuroVector EA3400 Series CHNS-O analyzer with acetanilide as the reference. The oxygen content was determined by difference. All analyses were carried out at least in duplicate and the average value is reported.

2.3.2.5. Water content. The water content of the pyrolytic sugar feeds and the product oils were determined using a Karl-Fischer (Metrohm 702 SM Titrino) titration. About 0.01 g of sample was introduced to an isolated glass chamber containing Hydranal solvent (Riedel de Haen) by a 1 mL syringe. The titration was carried out using Hydranal titrant 5 (Riedel de Haen). Mili-Q water was assumed as water content 100% used to calibrate the results of titration. All analyses were carried out at least in duplicate and the average value is reported.

2.3.2.6. Gel permeation chromatography (GPC). GPC analyses of the organic products were performed using an Agilent HPLC 1100 system equipped with a refractive index detector. Three columns in series of mixed type E (length 300 mm, i.d. 7.5 mm) were used. Polystyrene was used as a calibration standard. 0.05 g of the organic phase was dissolved in 5 mL of THF (10 mg/mL) together with 2 drops of toluene as the marker and filtered (pore size 0.2 μm) before injection.

2.3.2.7. Thermogravimetric analysis (TGA). TGA analysis of the pyrolytic sugar feeds, the product oils and spent catalysts were determined using a TGA 7 from Perkin-Elmer. The samples were heated in a nitrogen atmosphere with a heating rate 10 °C/min and a temperature range between 20 and 900 °C.

2.3.2.8. Gas chromatography/mass spectrometry (GC–MS). GC–MS analyses of the liquid products were performed on a Hewlett-Packard 5890 gas chromatograph equipped with a quadrupole Hewlett-Packard 6890 MSD selective detector and a 30 m × 0.25 mm, i.d. and 0.25 μm film sol-gel capillary column. The injector temperature was set at 250 °C. The oven temperature was kept at 40 °C for 5 min, then increased to 250 °C at a rate of 3 °C/min, and then held at 250 °C for 10 min. Di-*n*-butyl ether was used as an internal standard for quantification of relevant components in pyrolytic sugars.

2.4. Catalysts characterization

2.4.1. Nitrogen physisorption analyses

Nitrogen physisorption analyses (− 196.2 °C) were carried out using a Micromeritics ASAP 2420 device. The samples were degassed in vacuum at 350 °C for 10 h. The surface area was calculated using the standard BET method (S_{BET}). The single point pore volume (V_T) was estimated from the amount of gas adsorbed at a relative pressure of 0.98 in the desorption branch. The pore size distributions (PSD) were obtained by the BJH method using the adsorption branch of the isotherms, while the t-plot method was employed to quantify the micropores.

2.4.2. CO chemisorption

The metallic surface area of the catalyst in reduced state was determined by CO pulse chemisorption measurements using a Chemosorb analyzer (Modern laboratory equipment, Novosibirsk, Russia). 50 mg of fresh catalyst was placed inside an U-shaped quartz reactor and heated to the preset temperature (350 °C for Ni-Cu, Ni-Pd, Ni-Pd-Cu catalysts and 400 °C for Ni, Ni-Mo, and Ni-Mo-Cu catalysts, heating rate 40 °C/min) under a flow of H_2 (30 mL/min). When the final temperature was reached, the reactor was purged by an inert gas (He) followed by cooling to RT. Subsequently, pulses of CO were fed to the reactor (100 μL) until the amount of CO in the outlet was constant according to thermal conductivity detector (TCD). Thereafter the amount of chemisorbed CO was estimated.

2.4.3. Transmission electron microscopy (TEM)

A Philips CM12 instrument equipped with a high-resolution camera was used to acquire and elaborate TEM images. Powdered samples were dispersed in 2-propanol under ultrasound irradiation and the resulting suspension was placed drop-wise on a holey carbon-coated support grid.

2.4.4. Scanning electron microscope with energy dispersive X-ray spectroscopy (SEM-EDX)

The morphology of the samples was investigated by scanning electron microscopy (SEM-EDX) using a Philips XL-30-FEG SEM at an accelerating voltage of 5 kV. Prior to analyses, the samples were treated with Au using a gold sputter coater device. EDX analysis was carried out by using samples without a pretreatment.

3. Results and discussion

3.1. Pyrolytic sugar (PS) analysis

The PS used in this study was prepared by the addition of water to a typical PL obtained from pine wood using a fast pyrolysis process. This results in the precipitation of the pyrolytic lignin fraction, which was separated, leaving an aqueous PS fraction. The PS feeds were analyzed in detail using various analytical techniques (elemental analysis (EA), GPC, HPLC and GC–MS). The elemental composition is given in Table 1, an overview of HPLC and GC–MS data is given in Table 3.

The main individual components are levoglucosan (16.0 wt%), glycolaldehyde (10.8 wt%) and water (14.5 wt%). The former two are well known components in pyrolysis liquids and sugar fractions derived thereof. In addition, GC–MS revealed the presence of a small amount of organic acids (2.5 wt%, mainly acetic acid) and ketones (1.4 wt%, hydroxyacetone, 2(5H)-furanone). In addition, small amounts of phenolics (0.4 wt%, phenol, 2-methoxy phenol) were present. A representative GC–MS spectrum is given in Fig. 1.

Table 3
Main components of the pyrolytic sugar used in this study by HPLC and GC–MS.

Sample preparation	Component in PS	Analysis method	Concentration (wt%)
None	Levoglucosan	HPLC	16.0
	Glycolaldehyde	HPLC	10.8
	Acids	GC–MS	2.5
	Ketones	GC–MS	1.4
	Phenolics	GC–MS	0.4
	Water	Karl-Fisher titration	14.5
	Total		45.6
Hydrolysis[a]	Glucose	HPLC	25.2
	Mannose/xylose	HPLC	7.8
	Arabinose	HPLC	0.4
	Total sugars		33.4

[a] Hydrolysis data are for an experiment at 80 °C (see experimental section for details).

When summing up the total of GC-HPLC detectable species, it is clear that a considerable amount of the PS fraction is not detectable by GC and HPLC (up to 55 wt%, see Table 3) and likely consists of higher molecular weight components. This was indeed confirmed by GPC measurements, see Fig. 2 for details.

The PS feed shows a relatively broad distribution with a sharp peak at lower molecular weights. The latter peak is likely associated with the presence of LG. This was confirmed by the addition of LG to a product sample followed by GPC analysis, resulting in an increase in the area of this particular peak. The higher molecular weight fraction likely consists of oligo-(anhydro)sugars.

To gain insight in the composition and the amount of hydrolysable sugars, the PS fraction was hydrolysed using dilute sulfuric acid at 80 and 120 °C for 24 h. At 80 °C, 25.2 wt% of glucose, 7.8 wt% of mannose/xylose and 0.4 wt% of arabinose were detected in the hydrolysate as shown in Table 3. The glucose is formed both from the hydrolysis of LG as well as from the oligomeric sugars. Thus, part of the PS oligomers is hydrolysable to monomeric sugars (glucose, mannose, xylose, arabinose). A hydrolysis experiment at 120 °C for 24 h gave very similar results, see Table S1 (Supporting information).

The total amounts of monomeric sugars in the PS fraction as detected after hydrolysis (80 °C) by HPLC is 33.4 wt%. This value is

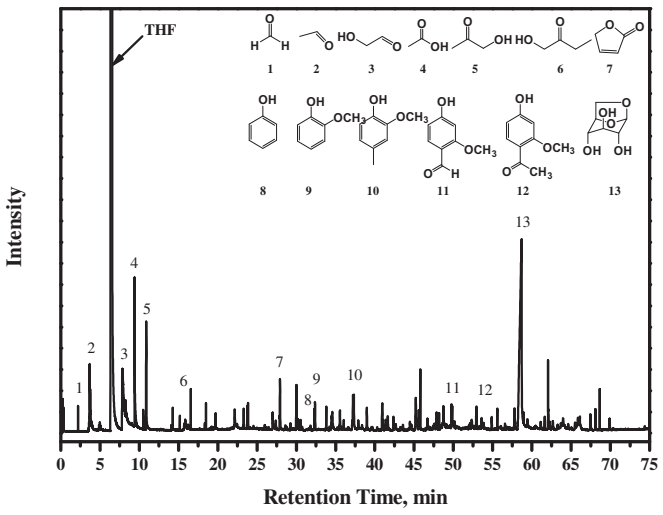

Fig. 1. Representative GC–MS spectrum of the PS feed.

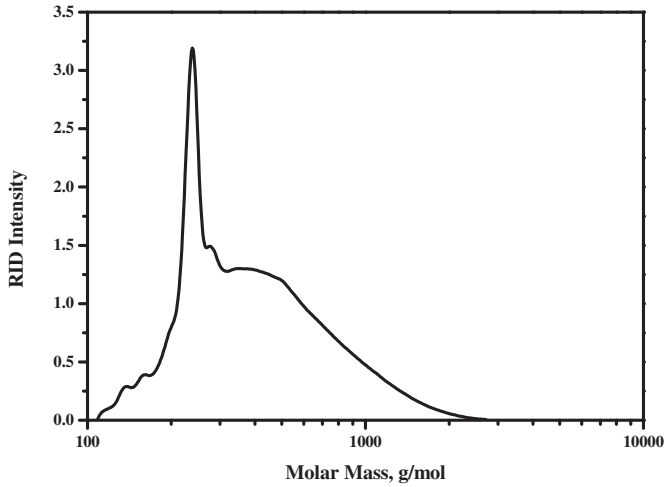

Fig. 2. Molecular weight distribution of the PS feed by GPC.

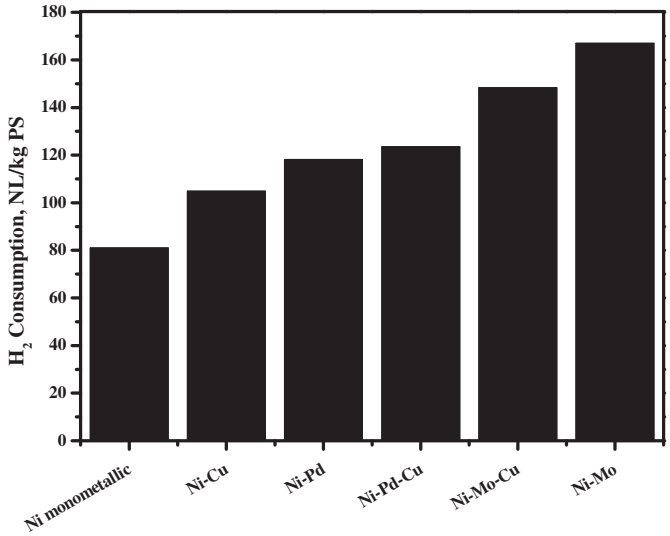

Fig. 3. Catalyst activity, expressed as hydrogen consumption on PS intake, for the various catalysts (batch, 180 °C, 4 h).

comparable with the value reported for PS obtained by fractional condensation of pyrolysis vapors by Li et al. (34.8 wt% [25]) and slightly lower than by Chi et al. (42 ± 2 wt% [26]).

3.2. Catalysts screening experiments in a batch set-up

Catalytic screening experiments were performed in a batch set-up at 180 °C for 4 h. All catalysts, except the monometallic Ni catalyst, yielded a single liquid phase product (94 to 99 wt% on PS intake) with a reddish brown colour for Ni-Cu, Ni-Pd, Ni-Pd-Cu catalysts and a dark brown colour for the Ni-Mo-Cu and Ni-Mo catalysts. An experiment with the monometallic Ni catalyst yielded two liquid phases, a water-rich top phase, an organic bottom phase and a sticky, viscous layer on the reactor wall. The amounts of gas, liquid and solid phase for each experiment are summarized in Table 4.

Minor amounts of gas phase components (0.6 to 1.4 wt% on PS intake) are formed, the major one being CO_2 (1.9–3.4 mol%). Likely, CO_2 is formed by decarboxylation reactions of small organic acids [27], which were shown to be present in the PS fraction (around 2.5 wt%, see Table 3). Methane and higher alkanes were not observed, indicating that the hydrogen is consumed solely for liquid phase reactions. Total mass balance closures are very satisfactory and above 95% for all experiments. Solids formation is limited (0–1.2 wt%), implying that thermal repolymerization does not occur to a considerable extent.

Table 4
Overview of results for the catalytic hydrotreatment of pyrolytic sugars.[a]

Catalyst	Ni	Ni-Cu	Ni-Pd	Ni-Pd-Cu	Ni-Mo-Cu	Ni-Mo
Liquid phase (wt% on PS intake)	99.1[b]	95.5	94.2	95.9	96.8	99.2
Solid (wt% on PS intake)	0.05	0.03	0.00	0.04	0.43	1.21
Gas phase (wt% on PS intake)	1.4	1.3	1.2	1.2	0.6	0.6
Carbon dioxide (mol%)	3.4	3.1	3.1	3.1	1.9	2.1
Hydrogen (mol%)	96.6	96.9	96.9	96.9	98.1	97.9
Formation of a separate water phase	Yes	No	No	No	No	No
Water content in liquid phase (wt%)	26.1[c]	24.2	22.7	21.0	21.1	20.1
Amount of water formed (wt % on dry PS intake)	13.6	11.4	9.6	7.7	7.8	6.6
Mass balance closure	101	97	95	97	98	101
Hydrogen uptake (NL/kg PS)	81	105	118	124	148	167

[a] Reaction conditions: 5 wt% catalyst on PS intake, 120 bar H_2 (room temperature), 180 °C, 4 h.
[b] Two liquid phases.
[c] Average value for the two liquid products.

3.3. Catalyst activity

Since CO_2 is the sole product in the gas phase and methane and higher alkanes are absent (Table 4), all the hydrogen consumed is used for hydrogenation reactions. As such, the experimentally measured hydrogen uptake during a reaction is a good measure for catalyst activity and the results are given in Fig. 3. Lowest activity was found for the monometallic Ni catalyst (81 NL/kg_{feed}) whereas the bimetallic Ni-Mo catalyst is the most active (167 NL/kg_{feed}). Thus, a clear promoting effect of the second metal is observed. The addition of Cu to the monometallic Ni catalyst lead to higher hydrogenation activity [28,29], whereas the addition of Pd (in both Ni-Pd and Ni-Pd-Cu) gave a further improvement. Thus, Pd seems is a better promoter in these reactions than Cu, which is in agreement with results obtained for pyrolysis liquids [13].

Promotion by Mo gave the best results and the highest hydrogenation activity was found for a bimetallic Ni-Mo catalyst. Thus, Mo is a better promotor for these Ni-based catalysts than Cu. Comparison with Pd is not well possible as considerably lower amounts of Pd were used in the catalyst formulation compared to Mo (Table 2).

3.4. Product analysis

All the liquid product phases were analyzed by elemental analysis and the data are provided in a van Krevelen plot given in Fig. 4. For reference, the data for the PS feed, the theoretical dehydration line and the results for a non-catalytic experiment are displayed as well. The latter was performed with PS and nitrogen in the absence of a catalyst. This led to the formation of large amounts of solids and a very viscous black organic phase (less than 5 wt%). In this case, polymerization of reactive molecules associated with water formation and the formation of char/humin type materials is occurring to a significant extent (Scheme 1) [30].

The van Krevelen plot gives valuable insights in the reaction pathways occurring during the catalytic hydrotreatment, specifically on hydrogenation and reactions involving the formation of water (e.g. condensation, polymerization and alcohol dehydrations) [5]. The elemental composition of the product oils is a clear function of the type of catalyst used. The O/C ratio varies between 0.40 and 0.51, whereas the H/C ratio spans a much larger range and is between 1.36 and 1.84.

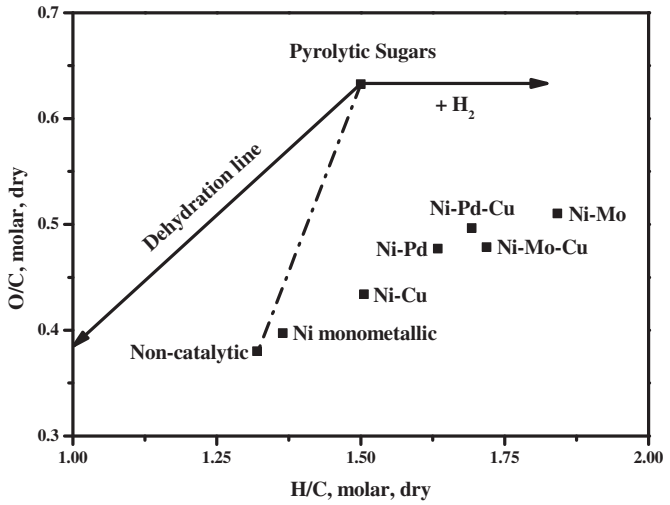

Fig. 4. Van Krevelen diagram of the pyrolytic sugar and its products (all on dry basis) after a catalytic hydrotreatment reaction (4 h, 180 °C).

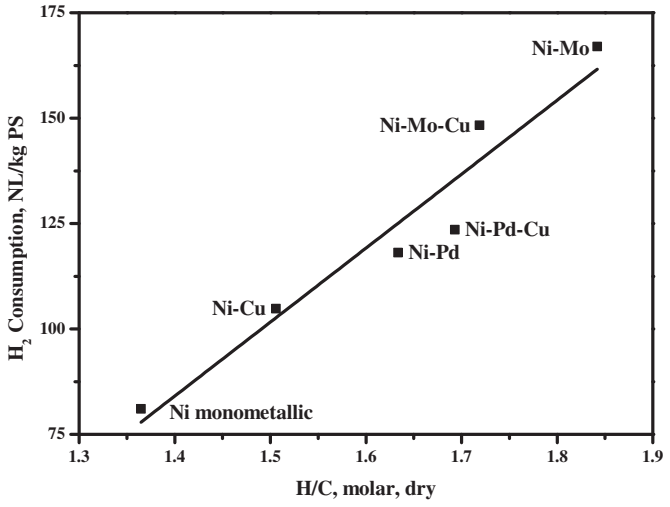

Fig. 5. Hydrogen consumption versus H/C ratio of the products for the various catalysts.

Products with a higher H/C ratio are associated with a high hydrogenation activity of the catalysts. This was confirmed by plotting the hydrogen consumption versus the H/C ratio for all product oils (Fig. 5). An almost linear relationship is observed, with higher H_2 consumptions yielding products with higher H/C molar ratios. Thus, the H/C ratio of the product is indeed a good quantitative measure for catalytic activity.

For the monometallic Ni catalyst, the hydrogen uptake and the H/C and O/C molar ratio are the lowest within the series. Surprisingly, the elemental ratios (H/C and O/C) are even lower than for the PS feed. The result for a non-catalytic run with the PS feed is also given in Fig. 4. Here, two separate liquid phases were obtained, a very viscous bottom organic phase and an aqueous phase top layer. The elemental composition of the product oil from the monometallic Ni catalyst is close to that of the non-catalytic experiment. As such, the data indicate that the monometallic Ni is not a very active catalyst for the catalytic hydrotreatment of PS, in line with the low hydrogen uptake (Fig. 3). In addition, the low H/C ratio for the monometallic Ni catalyst is indicative for the occurrence of dehydration reactions (see theoretical dehydration line in Fig. 4), leading to higher molecular weight products. The latter is supported by molecular weight determinations (see GPC, vide infra, Fig. 7) and the amounts of water produced during the hydrotreatment procedure.

All other catalysts lead to the formation of a single organic phase

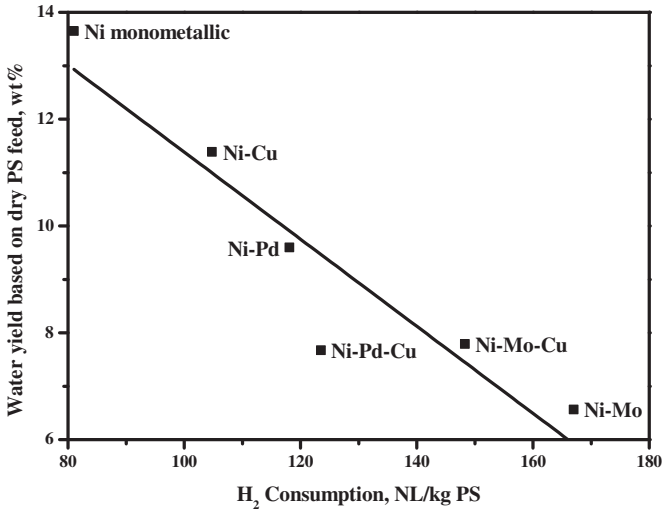

Fig. 6. Yield of water (wt%) versus H_2 uptake of all the catalysts.

with H/C ratios similar or higher than the PS feed. However, the oxygen content is considerably lower. These findings indicate that dehydration is not the main reaction occurring and that hydrogenation reactions leading to higher H/C ratios, also play a major role.

The statement that the non-catalytic thermal repolymerization reactions particularly lead to the formation of water is supported by considering the water production during the hydrotreatment reaction (Table 4) versus the activity of the catalysts (Fig. 6).

Indeed, for the most active catalysts, the lowest amount of water is formed, implying that repolymerization reactions leading to water do not occur to a significant extent for these catalysts. It supports the hypothesis that these catalysts are very active for the hydrogenation of reactive compounds to stabilized compounds that are less prone to polymerization at relatively low temperature.

To determine the extent of polymerization during reaction, the molecular weight distributions of the organic products were analyzed by GPC and the results are given in Fig. 7. After the catalytic hydrotreatment reactions, the molecular weight of the products are slightly higher than for the starting PS feed, indicative for the occurrence of polymerization reactions during the catalytic hydrotreatment. As postulated before, this is likely due to thermal reactions involving the carbonyl groups of the various sugars and smaller aldehydes (glycolaldehyde, Table 3) and ketones present in the PS feed [30]. When considering the low molecular weight part of the distribution, the peak of LG (about 250 g/mol) is reduced considerably and a new peak at around 150–200 g/mol is formed. The latter is likely ethylene glycol (EG), which was confirmed by spiking the sample with pure EG. The latter may be formed by hydrogenolysis of LG [31].

A small but clear difference in the molecular weight distribution is found for the product oils obtained from the various catalysts (Fig. 7 top). The molecular weight increase is smallest for the Ni-Mo catalyst and highest for the Ni-Cu catalyst. For the monometallic Ni catalyst, the increase in molecular weight is more difficult to determine as two liquid phases are formed. However, the molecular weight of the organic phase is the highest of all, indicative for the occurrence of a high extent of polymerization reactions (Fig. S1, Supporting information).

The molecular weight increase is anticipated to be a function of the rate of polymerization versus hydrogenation, suggesting that a catalyst with the highest hydrogenation activity will give the smallest increase in molecular weight (Scheme 1). This hypothesis is indeed confirmed by plotting the activity of the catalyst, expressed in terms of H_2 uptake, versus the molecular weight of the product oil (Fig. 8). A clear trend is visible, with the most active catalyst (Ni-Mo) giving a product with the lowest molecular weight.

Based on these results, the Mo promoted catalyst is the best catalyst

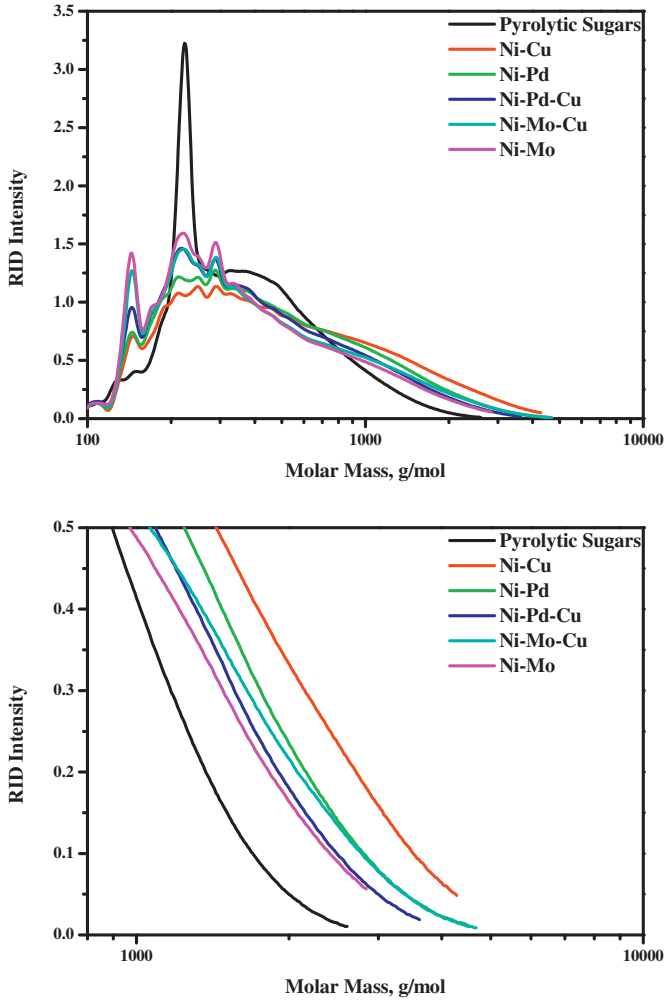

Fig. 7. Molecular weight distribution for the organic product oil for all catalysts except the monometallic Ni (top) and enlargement of the higher molecular weight tail (bottom).

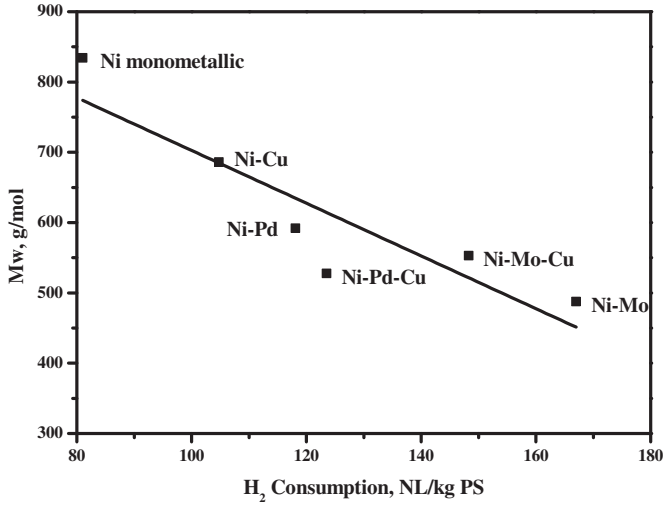

Fig. 8. Average molecular weight (Mw, g/mol) versus H_2 uptake (NL/kg PS) for all catalysts.

for the hydrotreatment of the pyrolytic sugars at the prevailing relatively mild reaction condition. It shows the highest hydrogen uptake, the highest H/C value of the product oil and the least increase in the amount of higher molecular weight components.

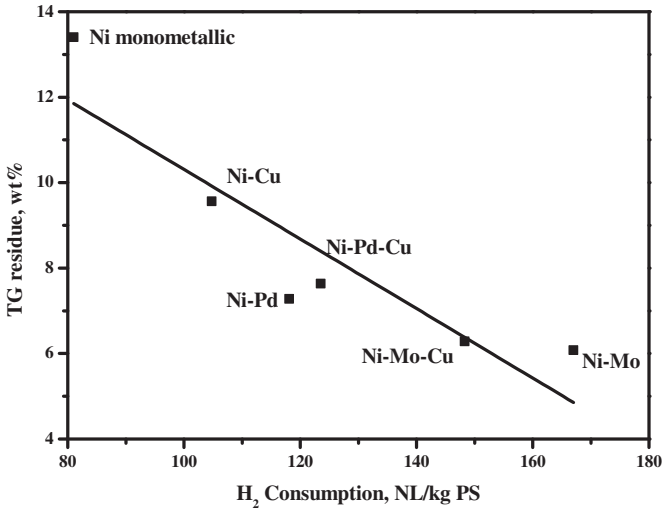

Fig. 9. TG residue versus H/C ratio of products for the catalysts used in this study.

The products were also analyzed by TGA to determine the residue after heating a sample to 900 °C. This residue (TG residue) is an indicator for the charring tendency of the liquid [13] (and as such related to the micro carbon residue test (MCRT) value conventionally used for crude oil feeds [32]). Products with a lower TG residue are preferred. The TG residues for the various products are plotted in Fig. 9; the TGA curves of the PS feed and a typical product using the Ni-Mo catalysts are shown in Fig. S2 (Supporting information). The TG residue of the products decreased from > 12 wt% for the original PS to values between 6 and 10 wt% for the product oils. For a non-catalytic run, the main product was a solid and only 10 wt% of a liquid phase was obtained. The TG residue of the solid phase was as high as 25 wt%, see Fig. S2 (Supporting information). The Ni catalyst with Mo as the promoter gave a product with the lowest TG residue. The TG residue of the products also correlates nicely with the activity of the catalysts in terms of H_2 uptake. As such, it implies that a higher hydrogenation activity leads to products with a lower charring tendency.

These findings can be rationalised considering that in particular the aldehydes and ketones are responsible for polymerization reactions and the formation of char. During the hydrotreatment process, aldehydes and ketones are converted to alcohols [33] (Scheme 2), examples are the conversion of glucose and LG to sugar alcohols such as hexitols [34,35] and diols [36,37]. These alcohols have a lower charring tendency than the aldehydes/ketones present in the original PS feed.

The reactivity of carbonyl compounds were confirmed by GC–MS measurements as shown in Fig. 10.

The original PS feed contains significant amount of carbonyl-containing molecules, e.g. aldehydes (formaldehyde, acetaldehyde, glycolaldehyde, etc.) and ketones (acetol, 2(5H)-furanone) as shown in Fig. 1 (vide supra). After hydrogenation at 180 °C for 4 h, aldehydes and ketones are absent in the product. Hydrogenation of carbonyl-containing molecules was further confirmed by ^{1}H-^{13}C NMR (Fig. 11). After

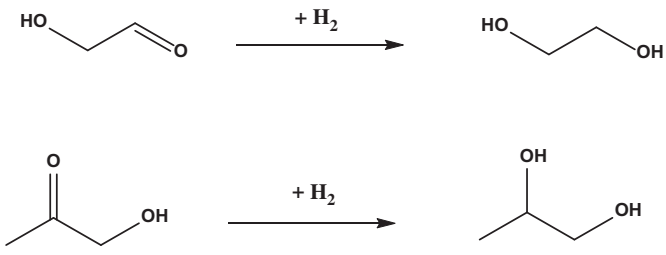

Scheme 2. Hydrogenation of two representative carbonyl-containing molecules in PS feed to alcohols.

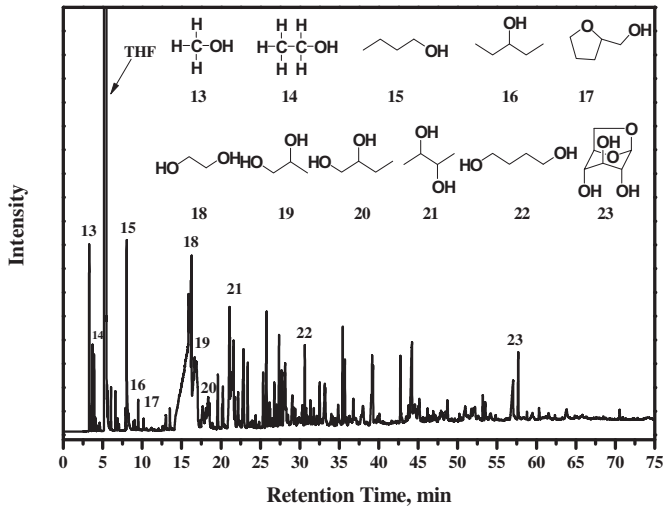

Fig. 10. Representative GC–MS spectrum of the hydrogenated PS using Ni-Mo catalyst.

hydrogenation at 180 °C for 4 h, the carbonyl compounds are fully converted, in agreement with the GC–MS results.

It is of interest to notice that the conversion of LG is far from quantitative and considerable amounts of LG are detected in the product. As such, the hydrolysis of LG to glucose and the subsequent hydrogenation of glucose to among others sorbitol is relatively slow on the timescale of the reaction under the prevailing reaction conditions with the Ni-Mo catalyst.

Table 5
CO chemisorption data for both catalysts.

Catalyst	S_{AC}, $m^2\ g_{cat}^{-1}$	μmol CO g_{cat}^{-1}
Ni	16.3	416
NiMo	13.2	337

Samples were pre-treated at 400 °C prior to the measurement, the details are given in Section 2.4.

3.5. Catalysts characterization

Detailed catalyst characterization studies for the fresh catalysts used in this study are given in Ref. [38]. Here, we report additional measurements (N_2 physisorption data and CO chemisorption data) for the most active (Ni-Mo/SiO_2-Al_2O_3) and the least active catalyst (Ni/SiO_2-Al_2O_3). In addition, the spent catalysts after reaction were also analyzed to gain insights in structural changes induced by the hydrotreatment reaction.

3.5.1. Characterization of the fresh catalysts

XRD and TPR studies [38] revealed that the oxidized NiMo catalyst contains isolated highly dispersed Mo oxides, as well as highly dispersed Mo oxides in intimate contact with NiO. Upon reduction at 400 °C, only part of the Ni is reduced and the highly dispersed Mo oxides in intimate contact with NiO likely form a NiMo solid solution. These bimetallic species may be more active than monometallic ones and may explain the experimentally observed higher activity of the NiMo catalyst compared to the monometallic one. However, it is also well possible that Mo in intermediate oxidation states have (in combination with Ni) a positive effect on activity by activation of oxygenated species. Evidence for the latter has been reported for the

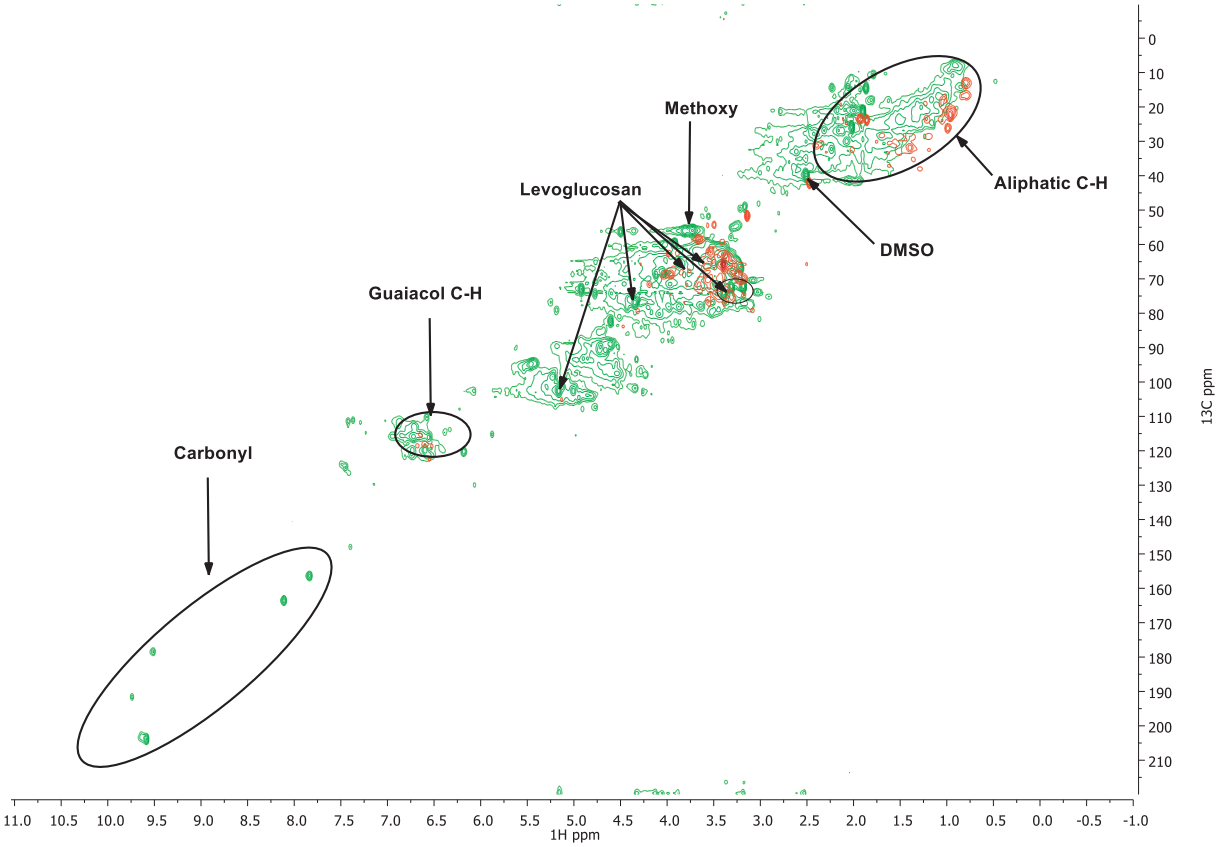

Fig. 11. Heteronuclear Single Quantum Coherence (HSQC) spectra of PS and hydrogenated PS using Ni-Mo: PS (green) and hydrogenated PS (red). (For interpretation of the references to colour in this figure legend, the reader is referred to the web version of this article.)

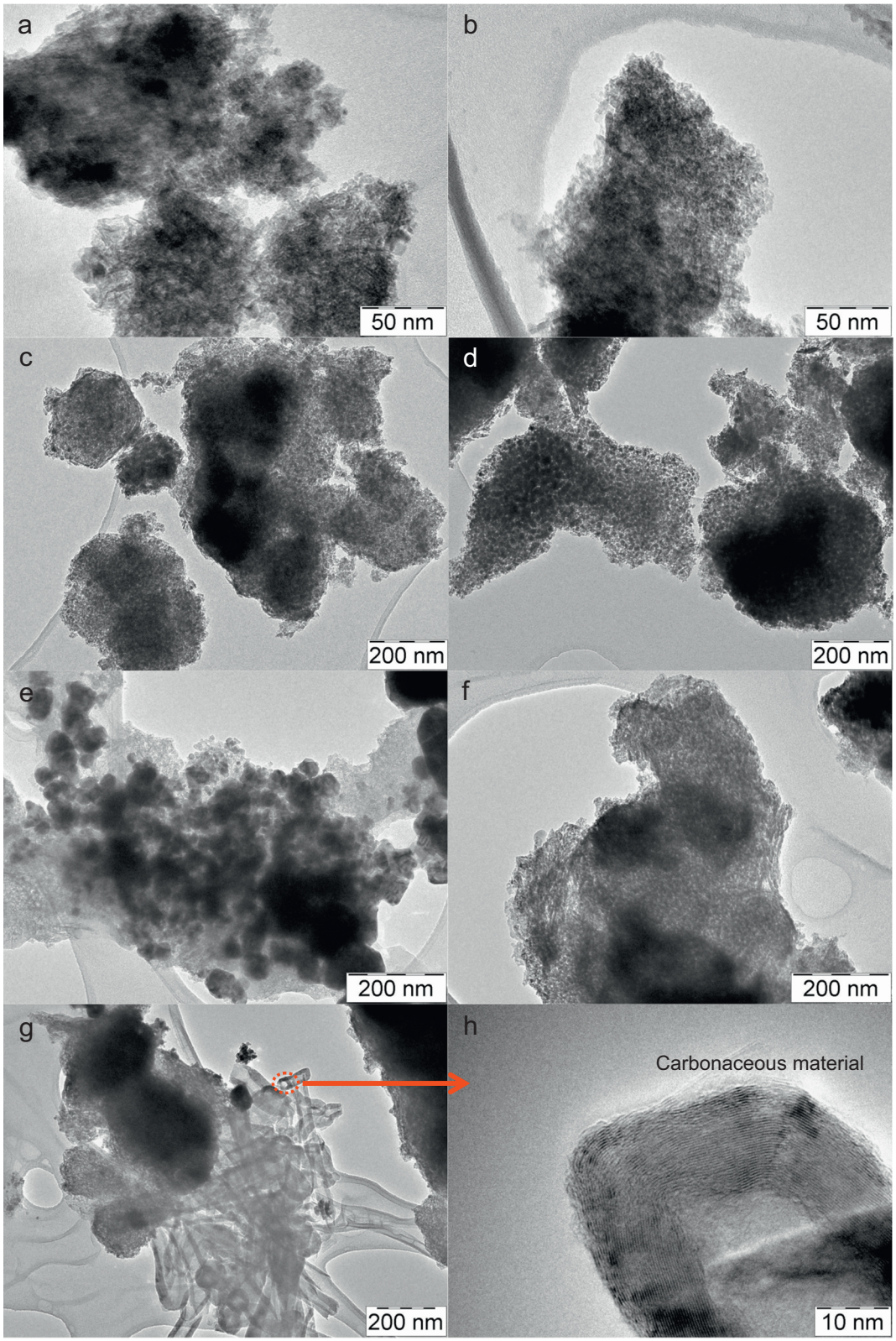

Fig. 12. TEM images of the monometallic Ni and bimetallic Ni-Mo catalyst before and after reaction at 180 °C: a) fresh monometallic Ni catalyst, oxidized form, b) fresh Ni-Mo catalyst, oxidized form, c) fresh monometallic Ni catalyst, reduced form, d) fresh Ni-Mo catalyst, reduced form, e) spent monometallic Ni catalyst, f) spent Ni-Mo catalyst, g) spent Ni-Mo catalyst, h) magnification of a selected area in spent Ni-Mo catalyst.

hydrodeoxygenation of esters using Mo supported Ni catalysts [39].

The N_2 adsorption-desorption isotherms of fresh Ni/SiO_2-Al_2O_3 and Ni-Mo/SiO_2-Al_2O_3 catalysts are provided in Fig. S3 (Supporting information). The BET surface area of fresh Ni/SiO_2-Al_2O_3 was 266 $m^2 \cdot g^{-1}$ whereas a slightly lower value for the Ni-Mo catalyst was observed (219 $m^2 \cdot g^{-1}$). These values are somewhat higher than reported in the literature for related catalysts (about 100–180 $m^2 \cdot g^{-1}$) [7,19,20,40]. These differences are likely due to the fact that the

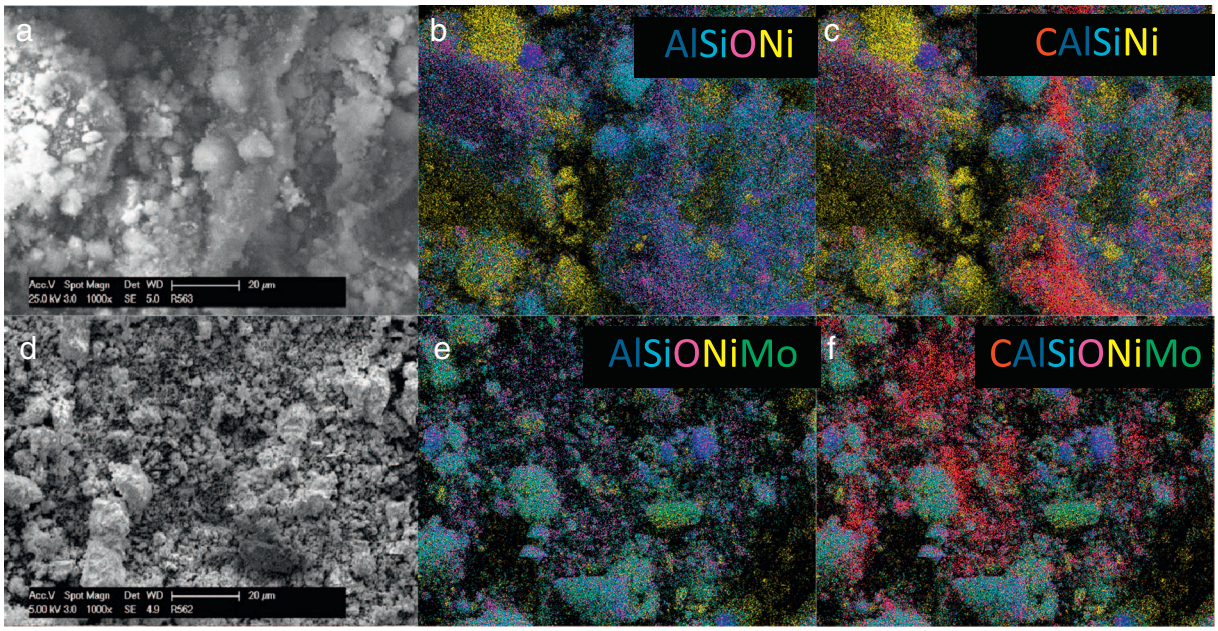

Fig. 13. SEM-EDX mapping investigations on spent catalysts: a), b), c) from spent Ni/SiO_2-Al_2O_3, d), e), f) from spent Ni-Mo/SiO_2-Al_2O_3.

catalysts in the present study were measured in their oxidized states.

CO chemisorption data obtained for the two reduced samples are given in Table 5. The reductive pretreatment procedure is given in Section 2.4. It is generally assumed that the use of CO as a probe molecule is advantageous for determination of active surface area of catalysts used in hydrotreatment processes. The specific surface areas of active component (S_{AC}) were calculated from the uptake of CO using the approach and assumptions used in [7]. In addition, it was assumed that CO is chemisorbed only by the metallic Ni species, though it is known that Mo^{x+} species also can contribute to CO adsorptions [41]. In this respect the absolute amount of chemisorbed CO given in Table 5 might be more reliable to compare the catalysts.

It is evident from Table 5 that the monometallic Ni-based catalyst shows a higher CO uptake than the bimetallic NiMo one. This is likely due to a higher extent of reduction of the monometallic Ni catalyst, confirmed by TPR measurements and XRD studies.

The TEM images of the fresh catalyst show lamellar structures with the metal nanoparticles uniformly distributed (Fig. 12a, b, c and d). This high dispersion of the metal nanoparticles is supported by the XRD data [38], showing broad peaks associated with a NiO and Ni phase. The presence of such highly dispersed metal nanoparticles in combination with the high metal loading explains the high catalyst activity for particularly the bimetallic Ni-Mo catalyst.

3.5.2. Characterization of the spent catalysts

The spent catalysts were analyzed using TEM and SEM-EDAX. Clear agglomeration of metal nanoparticles was observed for the monometallic Ni catalyst after the catalytic hydrogenation as shown in Fig. 12e. This is likely due to the high Ni loading on the catalyst (48%). Agglomeration is by far less for the bimetallic catalyst (Fig. 12f and g). As such, it is well possible that the addition of Mo has a positive effect on the stability of the metal nanoparticles and that sintering rates are reduced compared to the monometallic Ni catalyst. It also suggests that the Mo promoted catalyst is likely a more stable catalyst, though this needs to be verified in continuous set-ups for prolonged runtimes.

Some carbonaceous deposits were present on the Ni-Mo catalyst after reaction, see Fig. 12g and h. This probably due to the deposition of some higher molecular weight polymerization products from the polymerization of sugars in the PS feed, which was supported by GPC measurements (Fig. 7). The presence of carbonaceous deposits on the spent Ni and Ni-Mo catalysts was confirmed by TGA analysis under N_2 (Fig. S4, Supporting information). These measurements also show that the amounts of such deposits on the Ni catalyst are much higher than that for the Ni-Mo catalyst. The presence of carbonaceous deposits on both catalysts was confirmed by SEM-EDX measurements as shown in Fig. 13. Larger coke agglomerates on the Ni/SiO_2-Al_2O_3 catalyst (c) are detected, while in the presence of Mo (f), coke is indeed present but it is distributed more uniform.

Thus, we can conclude that the deposition of carbonaceous products and sintering, particularly for the monometallic catalyst occurs during the hydrotreatment reaction. These findings may affect catalyst activity considerably. Studies in continuous set-ups are in progress to determine the catalyst stability for prolonged runtimes.

4. Conclusions

The catalytic hydrotreatment of the PS fraction of pyrolysis liquids was studied at relatively low temperature (180 °C) using mono- and bimetallic Ni based catalysts characterized by a high amount of Ni. Catalyst screening experiments revealed that Mo addition to the nickel based catalyst gives the most active catalysts. Product analysis reveals that hydrogenation occurs to a significant extent and that thermal repolymerization is reduced considerably for this catalyst. As such, these findings support the statement that active hydrogenation catalysts at low hydrotreatment temperatures (< 200 °C) are required to avoid excessive polymerization of mainly small aldehydes, ketones and other low molecular weight C5 and C6 sugars, ultimately leading to char.

Catalyst characterization studies revealed that the NiMo catalyst contains small metal nanoparticles with a certain amount of a NiMo solid solution, which could be the reason for the high activity of this catalyst. Alternatively, the Ni nanoparticles in combination with Mo^{x+} species may also have a positive effect on catalyst activity as the latter are known to be able to activate oxygenated molecules. Metal agglomeration was shown to be a possible source for catalyst deactivation. This was particularly evident for the monometallic Ni catalyst, whereas this effect was by far lower for the bimetallic Ni-Mo catalyst. As such, the presence of Mo appears to prevent Ni sintering. In addition, some coke deposition on the catalyst surface was detected by TEM and SEM-EDX. Further studies in a continuous set-up to assess catalyst stability in detail are in progress and will be reported in due course.

The results of this study will be valuable input for the development of efficient catalytic hydrotreatment technologies for pyrolysis liquids involving a mild stabilization step followed by a deep hydrotreatment to obtain product oils with considerably reduced oxygen contents to be used as a co-feed in FCC units or as a blending component in biofuel. It appears that the Ni-Mo/SiO_2-Al_2O_3 catalyst reported here is a very promising catalyst for the 1st mild hydrotreatment step to obtain a stabilized product in high carbon efficiencies to be used as input for the second deep hydrotreatment step.

Acknowledgement

Financial support from Agentschap NL (BIORF01016) (Groene aardolie via pyrolyse, GAP) is gratefully acknowledged. R. M. Abdilla (Department of Chemical Engineering, University of Groningen) is acknowledged for sugar analysis. Hans van der Velde (Stratingh Institute for Chemistry, University of Groningen) is acknowledged for performing the elemental analyses and G. O. R. Alberda van Ekenstein (Department of Polymer Chemistry, Zernike Institute for Advanced Materials, University of Groningen) for TGA analysis. We also thank Qingqing Yuan, Jan Henk Marsman, Leon Rohrbach, Erwin Wilbers, Marcel de Vries and Anne Appeldoorn for analytical and technical support.

Appendix A. Supplementary data

Supplementary data to this article can be found online at https://doi.org/10.1016/j.fuproc.2017.10.006.

References

[1] J.N. Chheda, G.W. Huber, J.A. Dumesic, Liquid-phase catalytic processing of biomass-derived oxygenated hydrocarbons to fuels and chemicals, Angew. Chem. Int. Ed. 46 (2007) 7164–7183.
[2] G.W. Huber, S. Iborra, A. Corma, Synthesis of transportation fuels from biomass: chemistry, catalysts, and engineering, Chem. Rev. 106 (2006) 4044–4098.
[3] E. Taarning, C.M. Osmundsen, X. Yang, B. Voss, S.I. Andersen, C.H. Christensen, Zeolite-catalyzed biomass conversion to fuels and chemicals, Energy Environ. Sci. 4 (2011) 793–804.
[4] R.H. Venderbosch, W. Prins, Fast pyrolysis technology development, Biofuels Bioprod. Biorefin. 4 (2010) 178–208.
[5] R.H. Venderbosch, A.R. Ardiyanti, J. Wildschut, A. Oasmaa, H.J. Heeres, Stabilization of biomass-derived pyrolysis oils, J. Chem. Technol. Biotechnol. 85 (2010) 674–686.
[6] S. Czernik, A.V. Bridgwater, Overview of applications of biomass fast pyrolysis oil, Energy Fuel 18 (2004) 590–598.
[7] W. Yin, A. Kloekhorst, R.H. Venderbosch, M.V. Bykova, S.A. Khromova, V.A. Yakovlev, H.J. Heeres, Catalytic hydrotreatment of fast pyrolysis liquids in batch and continuous set-ups using a bimetallic Ni-Cu catalyst with a high metal content, Cat. Sci. Technol. 6 (2016) 5899–5915.
[8] W. Baldauf, U. Balfanz, M. Rupp, Upgrading of flash pyrolysis oil and utilization in refineries, Biomass Bioenergy 7 (1994) 237–244.
[9] A.R. Ardiyanti, A. Gutierrez, M.L. Honkela, A.O.I. Krause, H.J. Heeres, Hydrotreatment of wood-based pyrolysis oil using zirconia-supported mono- and bimetallic (Pt, Pd, Rh) catalysts, Appl. Catal. A Gen. 407 (2011) 56–66.
[10] J. Wildschut, F.H. Mahfud, R.H. Venderbosch, H.J. Heeres, Hydrotreatment of fast pyrolysis oil using heterogeneous noble-metal catalysts, Ind. Eng. Chem. Res. 48 (2009) 10324–10334.
[11] T.P. Vispute, H.Y. Zhang, A. Sanna, R. Xiao, G.W. Huber, Renewable chemical commodity feedstocks from integrated catalytic processing of pyrolysis oils, Science 330 (2010) 1222–1227.
[12] T.P. Vispute, G.W. Huber, Production of hydrogen, alkanes and polyols by aqueous phase processing of wood-derived pyrolysis oils, Green Chem. 11 (2009) 1433–1445.
[13] A.R. Ardiyanti, (PhD Thesis), University of Groningen. (2013). (ISBN: 978-94-6182-234-5).
[14] X. Zhang, L. Chen, W. Kong, T. Wang, Q. Zhang, J. Long, Y. Xu, L. Ma, Upgrading of bio-oil to boiler fuel by catalytic hydrotreatment and esterification in an efficient process, Energy 84 (2015) 83–90.
[15] X. Zhang, J. Long, W. Kong, Q. Zhang, L. Chen, T. Wang, L. Ma, Y. Li, Catalytic upgrading of bio-oil over Ni-based catalysts supported on mixed oxides, Energy Fuel 28 (2014) 2562–2570.
[16] X. Zhang, T. Wang, L. Ma, Q. Zhang, T. Jiang, Hydrotreatment of bio-oil over Ni-based catalyst, Bioresour. Technol. 127 (2013) 306–311.
[17] X. Zhang, Q. Zhang, T. Wang, B. Li, Y. Xu, L. Ma, Efficient upgrading process for production of low quality fuel from bio-oil, Fuel 179 (2016) 312–321.
[18] A.R. Ardiyanti, M.V. Bykova, S.A. Khromova, W. Yin, R.H. Venderbosch, V.A. Yakovlev, H.J. Heeres, Ni-based catalysts for the hydrotreatment of fast pyrolysis oil, Energy Fuel 30 (2016) 1544–1554.
[19] M.V. Bykova, D.Y. Ermakov, V.V. Kaichev, O.A. Bulavchenko, A.A. Saraev, M.Y. Lebedev, V.A. Yakovlev, Ni-based sol–gel catalysts as promising systems for crude bio-oil upgrading: guaiacol hydrodeoxygenation study, Appl. Catal. B Environ. 113–114 (2012) 296–307.
[20] M.V. Bykova, D.Y. Ermakov, S.A. Khromova, A.A. Smirnov, M.Y. Lebedev, V.A. Yakovlev, Stabilized Ni-based catalysts for bio-oil hydrotreatment: reactivity studies using guaiacol, Catal. Today 220–222 (2014) 21–31.
[21] V. A. Yakovlev, S. A. Khromova, D. Y. Ermakov, V. N. Parmon, R.H. Venderbosch, H.J. Heeres, A. R. Ardiyanti. Russian Patent 2,440,847, 2012.
[22] J. Lian, S. Chen, S. Zhou, Z. Wang, J. O'Fallon, C.-Z. Li, M. Garcia-Perez, Separation, hydrolysis and fermentation of pyrolytic sugars to produce ethanol and lipids, Bioresour. Technol. 101 (2010) 9688–9699.
[23] A.R. Ardiyanti, S.A. Khromova, R.H. Venderbosch, V.A. Yakovlev, H.J. Heeres, Catalytic hydrotreatment of fast-pyrolysis oil using non-sulfided bimetallic Ni-Cu catalysts on a δ-Al_2O_3 support, Appl. Catal. B Environ., 117–118 (2012) 105–117.
[24] A.R. Ardiyanti, S.A. Khromova, R.H. Venderbosch, V.A. Yakovlev, I.V. Melián-Cabrera, H.J. Heeres, Catalytic hydrotreatment of fast pyrolysis oil using bimetallic Ni–Cu catalysts on various supports, Appl. Catal. A Gen. 449 (2012) 121–130.
[25] X. Li, L.C. Luque-Moreno, S.R.G. Oudenhoven, L. Rehmann, S.R.A. Kersten, B. Schuur, Aromatics extraction from pyrolytic sugars using ionic liquid to enhance sugar fermentability, Bioresour. Technol. 216 (2016) 12–18.
[26] Z. Chi, M. Rover, E. Jun, M. Deaton, P. Johnston, R.C. Brown, Z. Wen, L.R. Jarboe, Overliming detoxification of pyrolytic sugar syrup for direct fermentation of levoglucosan to ethanol, Bioresour. Technol. 150 (2013) 220–227.
[27] B.J. O'Neill, E.I. Gürbüz, J.A. Dumesic, Reaction kinetics studies of the conversions of formic acid and butyl formate over carbon-supported palladium in the liquid phase, J. Catal. 290 (2012) 193–201.
[28] S.A. Khromova, A.A. Smirnov, O.A. Bulavchenko, A.A. Saraev, V.V. Kaichev, S.I. Reshetnikov, V.A. Yakovlev, Anisole hydrodeoxygenation over Ni–Cu bimetallic catalysts: the effect of Ni/Cu ratio on selectivity, Appl. Catal. A Gen. 470 (2014) 261–270.
[29] Y. Wang, T. Gao, Alloy formation and strength of Ni-Cu interaction in Ni-Cu/ZnO catalysts, React. Kinet. Mech. Catal. 70 (2000) 91–96.
[30] I. van Zandvoort, Y. Wang, C.B. Rasrendra, E.R.H. van Eck, P.C.A. Bruijnincx, H.J. Heeres, B.M. Weckhuysen, Formation, molecular structure, and morphology of humins in biomass conversion: influence of feedstock and processing conditions, ChemSusChem 6 (2013) 1745–1758.
[31] A.B. Bindwal, P.D. Vaidya, Kinetics of aqueous-phase hydrogenation of levoglucosan over Ru/C catalyst, Ind. Eng. Chem. Res. 52 (2013) 17781–17789.
[32] P. Ghetti, A rapid heating TGA method for evaluating the carbon residue of fuel oil, Fuel 73 (1994) 1918–1921.
[33] A.B. Bindwal, A.H. Bari, P.D. Vaidya, Kinetics of low temperature aqueous-phase hydrogenation of model bio-oil compounds, Chem. Eng. J. 207–208 (2012) 725–733.
[34] A. Fukuoka, P.L. Dhepe, Catalytic conversion of cellulose into sugar alcohols, Angew. Chem. 45 (2006) 5161–5163.
[35] H. Kobayashi, H. Ohta, A. Fukuoka, Conversion of lignocellulose into renewable chemicals by heterogeneous catalysis, Cat. Sci. Technol. 2 (2012) 869–883.
[36] R. Palkovits, K. Tajvidi, J. Procelewska, R. Rinaldi, A. Ruppert, Hydrogenolysis of cellulose combining mineral acids and hydrogenation catalysts, Green Chem. 12 (2010) 972–978.
[37] A.M. Ruppert, K. Weinberg, R. Palkovits, Hydrogenolysis goes bio: from carbohydrates and sugar alcohols to platform chemicals, Angew. Chem. Int. Ed. 51 (2012) 2564–2601.
[38] W. Yin, R.H. Venderbosch, S. He, M.V. Bykova, S.A. Khromova, V.A. Yakovlev, H.J. Heeres, Mono-, bi-, and tri-metallic Ni-based catalysts for the catalytic hydrotreatment of pyrolysis liquids, Biomass Convers. Biorefin. 7 (2017) 361–376.
[39] R.G. Kukushkin, O.A. Bulavchenko, V.V. Kaichev, V.A. Yakovlev, Influence of Mo on catalytic activity of Ni-based catalysts in hydrodeoxygenation of esters, Appl. Catal. B Environ. 163 (2015) 531–538.
[40] M.V. Bykova, O.A. Bulavchenko, D.Y. Ermakov, M.Y. Lebedev, V.A. Yakovlev, V.N. Parmon, Guaiacol hydrodeoxygenation in the presence of Ni-containing catalysts, Catal. Ind. 3 (2011) 15–22.
[41] C.C. Williams, J.G. Ekerdt, Infrared spectroscopic characterization of molybdenum carbonyl species formed by ultraviolet photoreduction of silica-supported molybdenum(VI) in carbon monoxide, J. Phys. Chem. 97 (1993) 6843–6852.